Sonic Hedgehog signaling impairs ionizing radiation–induced checkpoint activation and induces genomic instability

Jennifer M. Leonard,[1] Hong Ye,[2] Cynthia Wetmore,[1,2] and Larry M. Karnitz[3,4,5]

[1]Department of Biochemistry and Molecular Biology, [2]Department of Pediatrics and Adolescent Medicine, [3]Department of Molecular Pharmacology and Experimental Therapeutics, [4]Department of Radiation Oncology, and [5]Division of Oncology Research, College of Medicine, Mayo Clinic, Rochester, MN 55905

The Sonic Hedgehog (Shh) pathway plays important roles in embryogenesis, stem cell maintenance, tissue repair, and tumorigenesis. Haploinsufficiency of *Patched-1*, a gene that encodes a repressor of the Shh pathway, dysregulates the Shh pathway and increases genomic instability and the development of spontaneous and ionizing radiation (IR)–induced tumors by an unknown mechanism. Here we show that *Ptc1*$^{+/-}$ mice have a defect in the IR-induced activation of the ATR–Chk1 checkpoint signaling pathway. Likewise, transient expression of Gli1, a downstream target of Shh signaling, disrupts Chk1 activation in human cells by preventing the interaction of Chk1 with Claspin, a Chk1 adaptor protein that is required for Chk1 activation. These results suggest that inappropriate Shh pathway activation promotes tumorigenesis by disabling a key signaling pathway that helps maintain genomic stability and inhibits tumorigenesis.

Introduction

The Sonic Hedgehog (Shh; in vertebrates) signaling pathway, which was originally identified in *Drosophila melanogaster*, is highly conserved and plays critical roles in embryonic development in multiple organisms, including humans (Hooper and Scott, 2005). In addition to its pivotal role in embryogenesis, aberrant activation of Shh signaling is associated with tumorigenesis in many organs including skin, brain, lung, breast, prostate, and the pancreas (Jacob and Lum, 2007). The Shh pathway was first linked to tumor development in patients with basal cell nevus syndrome (BCNS; also known as Gorlin syndrome), who carry germline mutations in one allele of the *Patched-1* (*PTCH1*) gene (Hahn et al., 1996; Johnson et al., 1996). *PTCH1* encodes PTCH1, a transmembrane receptor that binds to and represses the activity of Smoothened (SMOH; Hooper and Scott, 2005). In normal cells, Shh signaling is initiated by the binding of the Shh ligand to PTCH, which relieves PTCH-mediated repression of SMOH (Hooper and Scott, 2005). In cells carrying a mutated *PTCH1* allele, SMOH signaling is inadequately repressed, leading to unrestrained activation of Gli1, a transcription factor and putative oncogene that is capable of inducing tumorigenesis in skin and brain (Ruiz i Altaba et al., 2007).

In addition to the predisposition for spontaneous tumorigenesis in BCNS patients, these patients are also at highly increased risk of tumor development in areas exposed to ultraviolet or ionizing radiation (IR; Gorlin, 1987). Similar to humans carrying mutation of *PTCH1*, deletion of one allele of *Ptc1* in mice (*Ptc1*$^{+/-}$) recapitulates these phenotypes, including an increased rate of spontaneous brain tumorigenesis (Goodrich et al., 1997; Wetmore et al., 2000) and a two- to fivefold increased incidence of medulloblastoma after exposure to IR (Hahn et al., 1998; Pazzaglia et al., 2002, 2006a). These observations suggest that aberrant Shh signaling in mice and humans increases genomic instability and compounds the tumorigenic effects of IR.

IR-induced double strand breaks (DSBs) activate the phosphatidylinositol 3-kinase–related kinases ATM and ATR, which regulate apoptosis, cell cycle progression, and DNA repair (Abraham, 2001). After the appearance of a DSB, ATM activates Chk2 and triggers the nucleolytic processing of the DSB into extended regions of single stranded DNA (ssDNA;

Correspondence to Larry M. Karnitz: karnitz.larry@mayo.edu; or Cynthia Wetmore: wetmore.cynthia@mayo.edu

Abbreviations used in this paper: BCNS, basal cell nevus syndrome; DSB, double strand break; HEK, human embryonic kidney; IR, ionizing radiation; MEF, mouse embryonic fibroblast; P, postnatal day; *PTCH1*, *Patched-1*; RPA, replication protein A; Shh, Sonic Hedgehog; SMOH, Smoothened; ssDNA, single stranded DNA.

The online version of this article contains supplemental material.

The Rockefeller University Press $30.00
J. Cell Biol. Vol. 183 No. 3 385–391
www.jcb.org/cgi/doi/10.1083/jcb.200804042

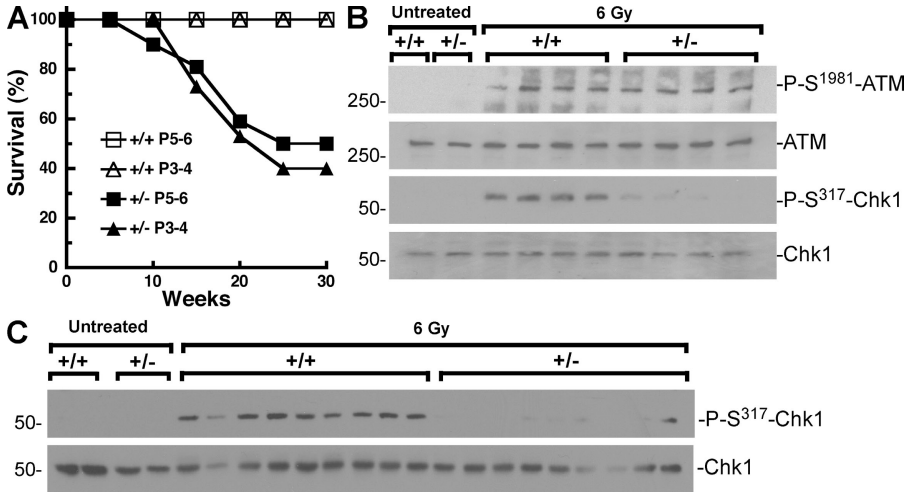

Figure 1. **DNA damage responses in wild-type and *Ptc1*$^{+/-}$ mice.** (A) Mice were exposed to 3 Gy IR and killed when they showed symptoms of increased intracranial pressure. Number of mice evaluated in each group is as follows: wild-type P3–4, $n = 8$; wild-type P5–6, $n = 16$; *Ptc1*$^{+/-}$ P3–4, $n = 19$; and *Ptc1*$^{+/-}$ P5–6, $n = 22$. The brain of each mouse was removed and inspected for the presence of tumor. All mice that died had a grossly apparent brain tumor in the cerebellum. (B and C) Wild-type and *Ptc1*$^{+/-}$ P5–6 mice were untreated or irradiated. 1 h later, the cerebella were dissected and lysed. Each lane represents the cerebellum from a separate mouse of the indicated genotype. Extracted proteins were immunoblotted for P-Ser^{1981}-ATM and P-Ser^{317}-Chk1. Membranes were reblotted with ATM and Chk1 antibodies, respectively. Molecular mass markers (in kilodaltons) are indicated on left sides of immunoblots.

Jazayeri et al., 2006). ATR is then activated when the ssDNA is coated by replication protein A (RPA), which recruits ATR (in a complex with ATR-interacting protein ATRIP) and triggers the loading of the Rad9–Hus1–Rad1 (9-1-1) complex. The 9-1-1 complex then induces ATR-mediated phosphorylation and activation of the protein kinase Chk1 (Zou, 2007) in a process that requires Claspin, an adaptor protein that is phosphorylated in an ATR-dependent manner. Once activated, Chk1 prevents cells from exiting G_2, regulates DNA repair, stabilizes stalled replication forks, and triggers the S-phase checkpoint (Bartek and Lukas, 2003). The importance of these pathways is underscored by the observations that they play critical roles in maintaining genomic stability (Liu et al., 2000; Weiss et al., 2000; Wang et al., 2003; Lam et al., 2004; Syljuasen et al., 2004; Durkin et al., 2006; Pandita et al., 2006) and in blocking the development of tumors (Bartkova et al., 2005; Gorgoulis et al., 2005).

Despite the longstanding observation that IR dramatically increases the incidence of tumors in BCNS patients and *Ptc1*$^{+/-}$ mice, how the Shh pathway influences tumorigenesis has remained elusive. Here we show that Shh pathway signaling attenuates activation of a genotoxin-triggered ATR–Chk1 checkpoint signaling pathway that serves as a barrier to the development of tumors.

Results and discussion

Ptc1$^{+/-}$ mice develop accelerated medulloblastomas after IR

To explore how dysregulated Shh signaling contributes to tumorigenesis, we first established an IR-induced model of tumorigenesis using *Ptc1*$^{+/-}$ mice. Previous studies demonstrated that irradiation of early postnatal *Ptc1*$^{+/-}$ mice on CDI/129 background dramatically increased the incidence of medulloblastoma, whereas irradiation at postnatal day (P) 10 or later did not increase the incidence of tumors above background (Hahn et al., 1998; Pazzaglia et al., 2002, 2006b). Because only limiting amounts of tissue are available for study in P3 mice, we asked whether *Ptc1*$^{+/-}$ mice on a C57Bl6/SvJ background developed medulloblastomas when irradiated at P5–6. Fig. 1 A shows that irradiated wild-type mice did not develop medulloblastomas over the 30-wk time course. In contrast, *Ptc1*$^{+/-}$ mice irradiated at P3–4 and P5–6 showed vastly increased rates of tumor incidence. Because irradiation of P3–4 and P5–6 *Ptc1*$^{+/-}$ mice led to comparable incidences of medulloblastoma, we used P5–6 animals for the studies that follow.

Ptc1$^{+/-}$ cerebella have a defect in Chk1 but not ATM activation

Defects in checkpoint signaling can lead to increased tumorigenesis, raising the possibility that the accelerated development of medulloblastomas in *Ptc1*$^{+/-}$ mice results from a defect in checkpoint signaling in developing cerebella. To address this possibility, we analyzed the activation of the ATM–Chk2 and ATR–Chk1 pathways in developing cerebellum after irradiation of wild-type and *Ptc1*$^{+/-}$ mice. Activation of the ATM pathway was assessed by immunoblotting dissected cerebella for phosphorylation of ATM on Ser^{1981}, a site that is autophosphorylated upon ATM activation (Bakkenist and Kastan, 2003). Activation of the ATR pathway was detected by phosphorylation of Chk1 on Ser^{317} and Ser^{345}, sites that are phosphorylated by ATR and required for Chk1 activation (Zhao and Piwnica-Worms, 2001). IR-induced ATM phosphorylation was equivalent in wild-type and *Ptc1*$^{+/-}$ cerebella (Fig. 1 B). In contrast, when compared with wild-type mice, IR-induced Chk1 phosphorylation on Ser^{317} was markedly reduced in the *Ptc1*$^{+/-}$ mice in two separate experiments (Fig. 1, B and C), as was phosphorylation of Chk1 Ser^{345} (Fig. S1 A, available at http://www.jcb.org/cgi/content/full/jcb.200804042/DC1). To rule out that differences in IR-induced Chk1 phosphorylation were the result of cell cycle redistribution in the *Ptc1*$^{+/-}$ cerebella, we analyzed cell cycle distributions in cells isolated from wild-type and *Ptc1*$^{+/-}$ mice. No difference was observed (Fig. S2 A). Collectively, these results demonstrate that the early postnatal cerebella of *Ptc1*$^{+/-}$ mice have a selective defect in IR-induced activation of the ATR–Chk1 signaling pathway, which may contribute to cellular transformation and tumorigenesis.

Gli1 disrupts Chk1 but not Chk2 activation in a model system

To develop a biochemically tractable model system to further investigate how Shh signaling impacts Chk1 activation, we reasoned

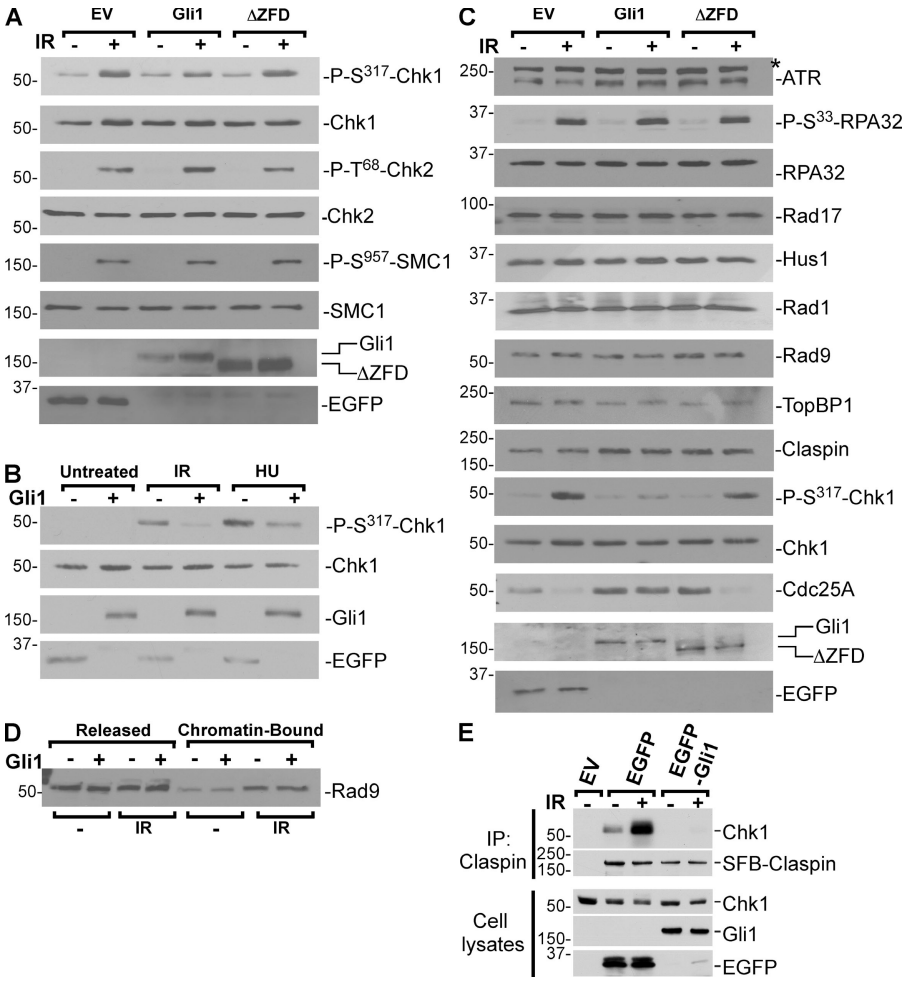

Figure 2. **Gli1 expression disrupts the ATR–Chk1 pathway.** (A and C) HEK293 cells were transfected with empty vector (EV), EGFP-Gli1 expression vector, or EGFP-Gli1$^{\Delta ZFD}$ expression vector and incubated for 20–24 h. Cells were left untreated (−) or exposed to 6 Gy IR and harvested 1 h later, and extracted proteins were immunoblotted as indicated. Asterisk indicates nonspecific antigen recognized by this antibody. (B) HEK293 cells transiently transfected with empty vector (−) or the EGFP-Gli1 expression vector (+) were treated with 6 Gy IR or 10 mM hydroxyurea. 1 h later the cells were harvested and extracted proteins were immunoblotted as indicated. Molecular mass markers (in kilodaltons) are indicated on the left side of immunoblots. (D) HEK293 transiently transfected with empty vector (−) or the EGFP-Gli1 expression vector (+) were treated with nothing (−) or 25 Gy IR and processed to separate unbound (Released) from chromatin-bound Rad9. Samples were then immunoblotted for Rad9. Molecular mass markers (in kilodaltons) are indicated on the left side of immunoblots. (E) HEK293 cells were transfected with empty vector (EV) and, as indicated, plasmids that encode EGFP, the EGFP-Gli1 expression vector, and SFB-Claspin. 24 h later, the cells were treated with nothing (−) or 6 Gy IR (+) and lysed 1 h later. SFB-Claspin was precipitated (IP) from cell lysates and the precipitates were washed and sequentially immunoblotted for Chk1 and S tag (to detect Claspin). Cell lysates were sequentially immunoblotted for Chk1 and EGFP (to show EGFP and EGFP-Claspin expression).

that expression of Gli1, a key mediator of the Shh pathway that is critical for medulloblastoma development (Kimura et al., 2005), would also affect Chk1 activation. Consistent with this hypothesis, Gli1 expression in human embryonic kidney (HEK) 293 cells suppressed IR-induced Chk1 Ser^{317} (Fig. 2 A) and Ser^{345} (Fig. S1 B) phosphorylation as well as the Chk1-dependent degradation of Cdc25A (Fig. 2 C). To rule out that this effect on Chk1 phosphorylation was the result of a Gli1-mediated disruption of the cell cycle, we analyzed the cell cycle profile of vector-transfected and Gli1-expressing cells. Gli1 did not disrupt cell cycle progression (Fig. S2 B).

To further characterize the effects of Gli1 on checkpoint signaling, we analyzed IR-induced Chk2 phosphorylation. Similar to what was observed in *Ptc1*$^{+/-}$ cerebella, Gli1 expression in HEK293 cells did not block the IR-induced phosphorylation of two ATM substrates, Chk2 and SMC1 (Fig. 2 A), thus demonstrating that Gli1 selectively blocks the ATR–Chk1 but not the ATM–Chk2 pathway. Notably, a Gli1 mutant (Gli1$^{\Delta ZFD}$) lacking the five zinc finger DNA-binding domains did not activate a Gli1-dependent promoter (not depicted) and did not suppress IR-induced Chk1 phosphorylation (Fig. 2 C), suggesting that Gli1 mediates its effect via transcription.

Although our results demonstrated that ATM phosphorylation of Chk2 and SMC1 was not compromised in Gli1-expressing cells, it was possible that Gli1 prevented ATM from generating the ssDNA intermediates that activate ATR. To address whether Gli1 affected the pathway upstream or downstream of ATR, we treated Gli1-expressing HEK293 cells with hydroxyurea, an agent that blocks DNA replication and induces ATR-mediated Chk1 phosphorylation that, unlike IR, does not require ATM (Feijoo et al., 2001). As was observed with IR, hydroxyurea-induced Chk1 phosphorylation was attenuated by Gli1 expression (Fig. 2 B). These results further confirm that Gli1 selectively disrupts the ATR–Chk1 signaling pathway in a manner distinct from ATM activation.

Gli1 interrupts the ATR–Chk1 pathway downstream of ATR

We next asked where Gli1 affected the Chk1 activation pathway. One of the first events in the pathway is the recruitment of the 9-1-1 complex to chromatin. As shown in Fig. 2 C, Gli1 did not affect the expression of Hus1, Rad1, and Rad9, the proteins that assemble into the 9-1-1 clamp (Volkmer and Karnitz, 1999), nor did it affect the expression of Rad17, the clamp loader for the 9-1-1 clamp (Zou, 2007). Consistent with these findings, Gli1 did not block the IR-induced binding of Rad9 (Fig. 2 D), a readout for the loading of the 9-1-1 complex at sites of DNA damage (Burtelow et al., 2000; Zou et al., 2002). Further examination of the ATR–Chk1 signaling pathway revealed that Gli1 expression also did not affect the levels of ATR or TopBP1 (Fig. 2 C),

nor did Gli1 block the IR-induced phosphorylation of RPA32 (Fig. 2 C), another ATR substrate (Olson et al., 2006). These results demonstrate that Gli1 does not block the early steps of the ATR signaling pathway or the ability of ATR to phosphorylate RPA32.

The ability of Gli1 to selectively disrupt Chk1 phosphorylation was similar to what has been observed when Claspin, a Chk1 adaptor protein, is depleted from human cells or *Xenopus laevis* egg extracts (Chini and Chen, 2004). Given these similar effects, we asked how Gli1 expression affected Claspin. Similar to the other checkpoint proteins, Claspin levels were not changed by Gli1 expression (Fig. 2 C) in HEK293 cells or by *Ptc1* status in mouse cerebella (Fig. S1 A). To further probe the effect of Gli1 on Claspin, we also assessed the impact of Gli1 expression on the DNA damage–induced interaction between Claspin and Chk1, an interaction that is critical for ATR-mediated Chk1 phosphorylation. Interestingly, we found that the IR-induced binding of Chk1 to Claspin (Fig. 2 E) was abolished by Gli1, suggesting that this transcription factor specifically disrupts the ability of Claspin to inducibly bind Chk1.

The Chk1-dependent activation of the S-phase checkpoint is disrupted by Gli1

To show the functional significance of Gli1-mediated disruption of Chk1 signaling, we examined activation of the S-phase checkpoint, a Chk1-dependent transient inhibition of DNA synthesis that is detected as a reduction in [^{3}H]thymidine incorporation into replicating DNA after IR treatment (Chen and Sanchez, 2004). As a positive control for these experiments, we used caffeine, an ATM/ATR inhibitor that disrupts the S-phase checkpoint in irradiated cells (Sarkaria et al., 1999). Consistent with reduced Chk1 phosphorylation in Gli1-expressing HEK293 cells, Gli1-expressing cells were as defective as caffeine-treated cells in activation of the S-phase checkpoint (Fig. 3 A).

Shh pathway activation sensitizes cells to IR

Chk1 facilitates the survival of irradiated cells, in part, by activating the S-phase checkpoint, preventing the progression from G2 to M phase, and activating DNA repair (Chen and Sanchez, 2004). Therefore, to further show that the reduced Chk1 phosphorylation seen in cells with an activated Shh pathway affects cellular responses, we examined cell survival after IR treatment using two cell systems. Irradiated mouse fibroblasts isolated from *Ptc1*$^{+/-}$ embryos demonstrated reduced survival in clonogenic assays compared with wild-type fibroblasts (Fig. 3 B). Similarly, transient expression of full-length Gli1 but not the zinc finger mutant Gli1$^{\Delta ZFD}$ decreased clonogenic survival in irradiated HEK293 cells (Fig. 3 C). Collectively, these results demonstrate that hyperactivation of the Shh pathway in mouse brains and HEK293 cells diminishes Chk1 phosphorylation and disrupts downstream cellular events that are dependent on Chk1.

Gli1 expression enhances IR-induced chromosome aberrations

Cells from BCNS patients show increased rates of IR-induced chromosome aberrations after radiation (Featherstone et al., 1983; el-Zein et al., 1995; Shafei-Benaissa et al., 1995, 1998). Similarly,

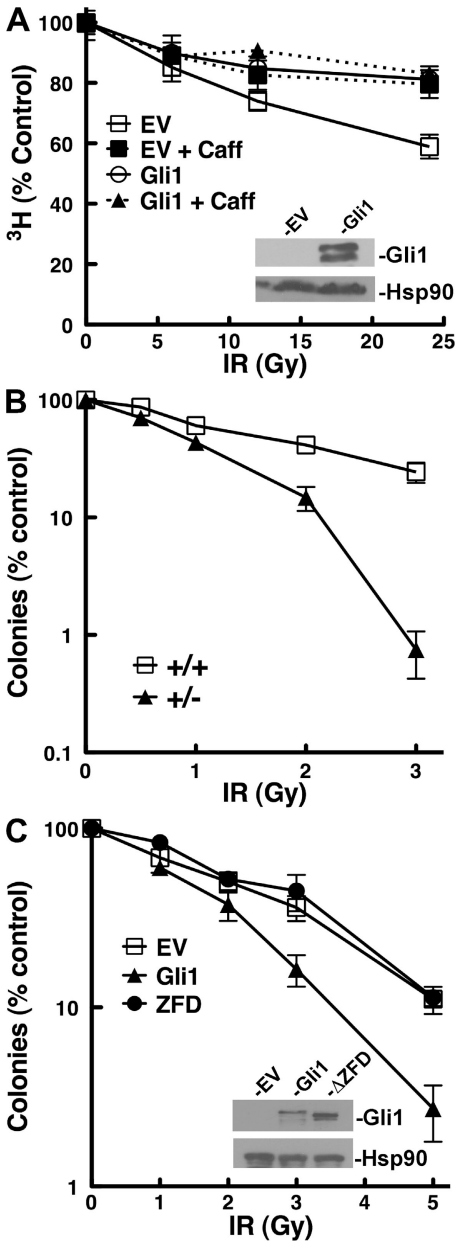

Figure 3. **Gli1 expression disrupts Chk1-dependent responses.** (A) S-phase checkpoint assay in HEK293 cells stably transfected with empty vector (EV) or EGFP-Gli1 (inset). 1 h before irradiation, the cells were treated with vehicle or 3 mM caffeine (Caff). Total counts per minute for the nonirradiated samples in each set were 20,400 ± 800 (EV), 20,900 ± 600 (Gli1), 15,400 ± 900 (EV + Caff), and 15,400 ± 700 (Gli1 + Caff). Data points show mean of three samples ± SD from one representative experiment. The experiment has been repeated four times with similar results. (B) Clonogenic assay of wild-type (+/+) or *Ptc1*$^{+/-}$ MEFs. MEFs (1,000 cells/well) were plated, irradiated, and incubated to allow colony formation. The plating efficiencies for wild-type and *Ptc1*$^{+/-}$ MEFs were 23.4 and 19.9%, respectively. Data points show mean of three samples ± SD from one representative experiment. The experiment has been repeated two times with similar results. (C) HEK293 cells transiently transfected with empty vector (EV), EGFP-Gli1, or EGFP-Gli1-ΔZFD (inset) were plated (300 cells/well, 0–3 Gy; 1,000 cells/well, 5 Gy), exposed to IR, and allowed to form colonies. Data points show mean of three samples ± SD from one representative experiment. Plating efficiencies for EV-, Gli1-, and Gli1-ΔZFD–transfected cells were 22.3, 20.4, and 16.7%, respectively. The experiment has been repeated three times with similar results.

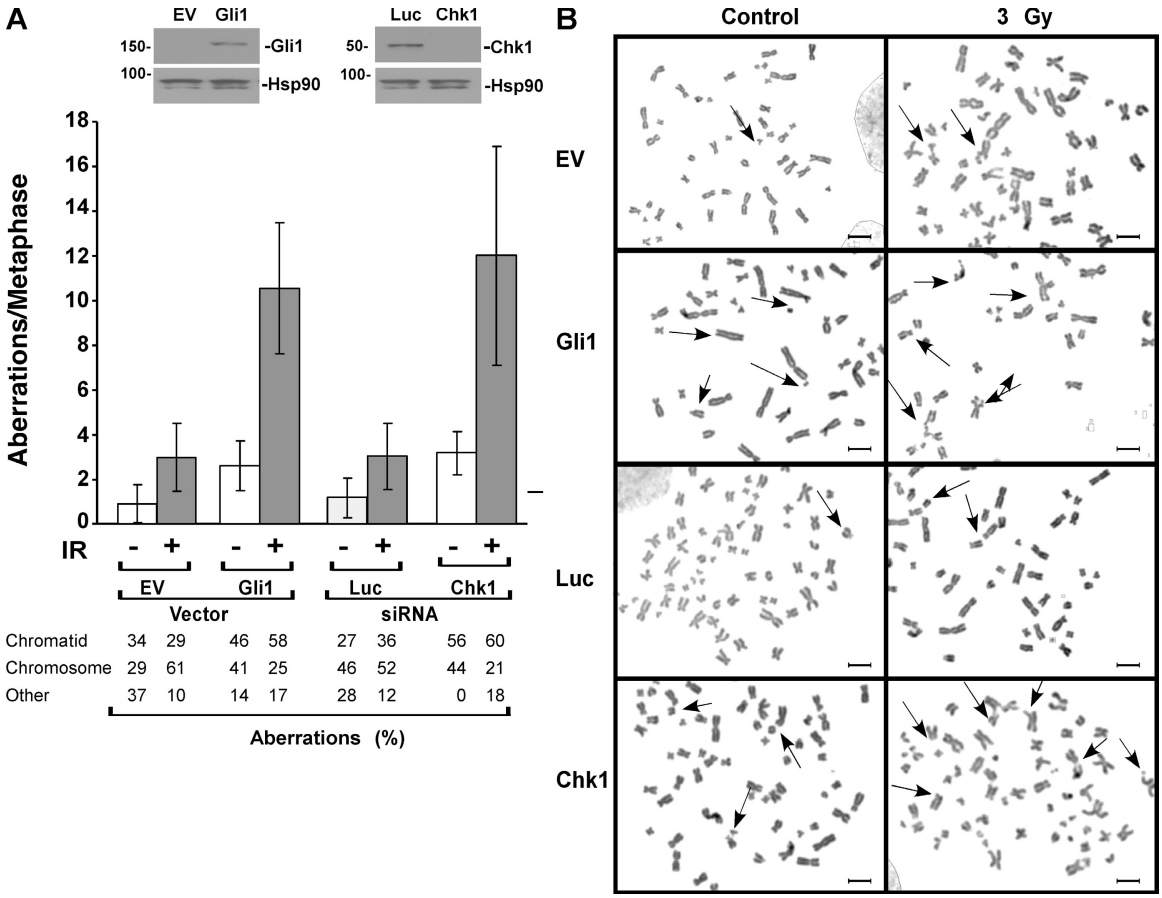

Figure 4. **Gli1 expression increases genomic instability.** (A) HEK293 cells were transiently transfected with empty vector (EV), the EGFP-Gli1 expression vector, or luciferase (Luc) siRNA or Chk1 siRNAs (insets above graph). Metaphases were scored for chromatid-type, chromosome-type, and other (dicentrics, rings, anaphase bridges, and pulverized chromosomes) aberrations. The graph shows the total number of aberrations counted in each sample. The breakdown (in percent) of each aberration type is shown in the data tabulated below the graph. Data points show mean of 20 cells ± SD. The experiment has been repeated three times with similar results. (B) Representative photomicrographs of samples quantitated in A. Bars, 5 µm. Arrows indicate aberrations.

disabling the ATR–Chk1 pathway at the level of Rad17, Rad9, ATR, or Chk1 leads to genomic instability (Weiss et al., 2000; Liu et al., 2000; Wang et al., 2003; Lam et al., 2004; Syljuasen et al., 2004; Durkin et al., 2006; Pandita et al., 2006). Because Shh signaling disrupts IR-induced Chk1 phosphorylation, we reasoned that Shh pathway activation might also affect the accumulation of IR-induced chromosome aberrations. To test this hypothesis, we expressed exogenous Gli1 in HEK293 cells. As a control, we also depleted Chk1 with siRNA. 24 h after irradiation, we analyzed the chromosomal aberrations by scoring for chromosome type, chromatid type, and other (dicentrics, rings, anaphase bridges, and pulverized chromosomes) aberrations (Fig. 4 A). Overall, there were large increases in all types of IR-induced aberrations in cells expressing Gli1 or depleted of Chk1 compared with control irradiated cells. Notably, however, when broken down by aberration type, both Gli1 expression as well as Chk1 depletion skewed the distribution of chromatid- versus chromosome-type aberrations so that chromatid-type aberrations became the dominant type of lesion when Chk1 signaling was attenuated by Gli1 expression or Chk1 depletion. Because chromatid breaks occur when cells are irradiated during S and G2, the results agree with previous studies showing that the ATR–Chk1 pathway is particularly important during these phases of the cell cycle, perhaps because ATR and Chk1 participate in the repair of DSBs by homologous recombination, a repair pathway that is particularly important during S and G2 (Petermann and Caldecott, 2006). Consistent with previously published findings, which showed that various components of the Chk1 pathway contribute to genomic stability (Liu et al., 2000; Weiss et al., 2000; Wang et al., 2003; Lam et al., 2004; Syljuasen et al., 2004; Durkin et al., 2006; Pandita et al., 2006), the present results demonstrate that hyperactivation of the Shh pathway contributes to genomic instability by attenuating Chk1 activation.

In the present study, we first demonstrate that there is a selective reduction in Chk1 activation in the cerebella of irradiated $Ptc1^{+/-}$ mice. We then show that expression of Gli1 in HEK293 cells phenocopies the reduced IR-induced Chk1 phosphorylation that was observed in irradiated $Ptc1^{+/-}$ mouse cerebella. Finally, we demonstrate that Gli1 disrupts the ATR–Chk1 pathway at the level of the IR-inducible interaction of Claspin and Chk1, and we show that this disruption in Chk1 activation leads to S-phase checkpoint defects and increases the accumulation of IR-induced chromosome aberrations. These results therefore suggest that Shh pathway activation may contribute to

medulloblastoma formation by attenuating the activation of a checkpoint that is important for maintaining genomic stability and that acts as a barrier to tumorigenesis. Moreover, given that the Shh pathway is implicated in the development of a wide range of human tumors (Jacob and Lum, 2007), these results raise the intriguing possibility that aberrant Shh signaling promotes tumorigenesis by attenuating Chk1 signaling and increasing genomic instability in other human tumors.

Materials and methods

Plasmids

The mouse *Gli1* coding sequence was amplified by PCR and cloned into pEGFP-C3 (Clontech Laboratories, Inc.) to create an EGFP-Gli1 expression vector. The zinc finger domains of Gli1 (amino acids 238–390) were deleted using the QuikChange kit (Stratagene) to create EGFP-Gli1$^{\Delta ZFD}$. The S- and FLAG-tagged Claspin expression vector (pSFB-Claspin; Chini and Chen, 2006) was provided by J. Chen (Yale University, New Haven, CT).

Animals, tissues, and tumor formation

Experimental protocols were approved by the Institutional Animal Care and Use Committee of the Mayo Clinic. Mice carrying deletion of exons 1 and 2 of *Ptc1* (*Ptc1*$^{+/-}$) mice were described previously (Goodrich et al., 1997). Animals were maintained on a mixed C57Bl6/129SvJ background.

The incidence of IR-induced medulloblastoma was assessed after irradiation of wild-type and *Ptc1*$^{+/-}$ mice with 3 Gy IR. Animals displaying ataxia, poor grooming, or severe malaise were killed, and brains were examined for medulloblastomas. Each brain was removed and examined for the presence of tumor. All mice that died during the period of observation had a grossly apparent brain tumor.

Cell culture and transfection

HEK293 cells were cultured in Dulbecco's modified Eagle's medium supplemented with 10% fetal bovine serum. For plasmid transfections, cells were electroporated as described previously (Volkmer and Karnitz, 1999) using a 225-V, 20-ms pulse. Luciferase (control) and Chk1 siRNAs were described previously (Karnitz et al., 2005) and transfected by electroporation using the same conditions used for plasmid transfections. HEK293 cells stably expressing EGFP-Gli1 were derived by Lipofectamine 2000 (Invitrogen) transfection with empty vector (pEGFP-C3) or the Gli1 (EGFP-Gli1) or Gli1$^{\Delta ZFD}$ (EGFP-Gli1$^{\Delta ZFD}$) expression vectors. Drug-resistant cells were selected in 500 µg/ml G418; >95% of the G418-resistant population was positive by GFP expression.

Clonogenic analysis

HEK293 or mouse embryonic fibroblast (MEF) cells were plated in 6-well dishes, allowed to adhere, and irradiated with a Shepard ^{137}Cs γ-irradiator. After 14 d, the plates were stained with crystal violet and colonies containing >25 cells were counted.

S-phase checkpoint and chromosome analyses

The intra–S-phase checkpoint was analyzed as described previously (Roos-Mattjus et al., 2003). For the chromosome aberration studies, HEK293 cells were transfected with empty vector or Gli1 expression plasmids or siRNA to luciferase or Chk1. 24 (plasmid transfections) or 48 h (siRNA transfections) later, the cells were irradiated, incubated for 24 h, treated with colcemid for 4 h, and fixed. Cells were deposited on slides and stained with Geimsa as described previously (Babu et al., 2003). Samples were randomized and visualized using a microscope (Axioplan 2; Carl Zeiss, Inc.) at 22°C. Images were acquired and analyzed using an Applied Images CytoVision workstation (Genetix). Chromosome aberrations were scored, in a blinded manner, for 20 cells per sample.

Western blotting, antibodies, Rad9 chromatin-binding assay, and Claspin–Chk1 interaction

HEK293 cells were lysed as described previously (Volkmer and Karnitz, 1999). Cerebella were dissected from adjacent tissues and triturated in lysis buffer used for HEK293 cells. Protein concentrations in lysates were determined using the Protein Assay kit (Bio-Rad Laboratories). Antibodies to the following antigens used in this study include: ATR (Genetex); phospho (P)-Ser^{1981}-ATM and P-Thr^{68}-Chk2 (R&D Systems); P-Ser^{317}-Chk1 and Chk2 (Cell Signaling Technology); Cdc25A (Thermo Fisher Scientific); RPA32, P-Ser^{33}-RPA32, P-Ser^{957}-SMC1, SMC1, and TopBP1 (Bethyl Laboratories); Chk1 (Santa Cruz Biotechnology, Inc.); GFP (Invitrogen); Gli1 (Rockland); P-H2AX (Millipore); and Rad17, Rad9, and Hus1 (Volkmer and Karnitz, 1999). Rad9 chromatin binding was performed as described previously (Burtelow et al., 2000). The Claspin–Chk1 interaction was analyzed in HEK293 cells that transiently expressed S- and Flagged-tagged Claspin as described previously (Chini and Chen, 2006).

HEK293 cell cycle analysis

HEK293 cells were transfected with empty vector or the EGFP-Gli1 expression vector. We also cotransfected an EGFP–histone H2B expression vector because fusion of EGFP to histone H2B anchors the EGFP in cells. This allowed us to analyze the cell cycle of the transfected cells and maintain the EGFP signal. 24 h after transfection, the cells were permeabilized in 0.1% sodium citrate containing 0.1% Triton X-100, 50 µg/ml propidium iodide, and 10 µg/ml heat-treated RNase A; incubated 30 min at 30°C; and analyzed for DNA content by flow cytometry.

Cerebellar granule cell cycle analysis

Cerebella were isolated and the cells were dissociated as described previously (Wang et al., 2000). The dissociated cells were prepared for cell cycle analysis using the Cycletest Plus kit (Becton Dickinson) and analyzed by flow cytometry to detect DNA content.

Online supplemental material

Fig. S1 shows that IR-induced Chk1 phosphorylation on Ser^{345} is disrupted in *Ptc1*$^{+/-}$ cerebella and in HEK293 cells expressing Gli1. Additionally, Fig. S1 shows that Claspin levels are not altered in *Ptc1*$^{+/-}$ cerebella. Fig. S2 demonstrates that cells from *Ptc1*$^{+/-}$ cerebella do not have an altered cell cycle compared with wild-type cells and that expression of EGFP-Gli1 does not affect cell cycle distribution in HEK293 cells. Online supplemental material is available at http://www.jcb.org/cgi/content/full/jcb.200804042/DC1.

We gratefully acknowledge Scott H. Kaufmann for insightful discussions, Junjie Chen for providing the SFB-Claspin expression vector and the Rad51 antibody, the Mayo Clinic Flow Cytometry/Optical Morphology Resource and the Cytogenetics Shared Resource for technical assistance, and Pam Becker for manuscript preparation.

This work was supported by CA-084321 (L.M. Karnitz), the Mayo Clinic Foundation (L.M. Karnitz and C. Wetmore), the Sontag Foundation, the Bernard and Edith Watermann Foundation for Cancer Genetics (C. Wetmore), and a Bonner Predoctoral Fellowship (J.M. Leonard).

Submitted: 8 April 2008
Accepted: 1 October 2008

References

Abraham, R.T. 2001. Cell cycle checkpoint signaling through the ATM and ATR kinases. *Genes Dev.* 15:2177–2196.

Babu, J.R., K.B. Jeganathan, D.J. Baker, X. Wu, N. Kang-Decker, and J.M. van Deursen. 2003. Rae1 is an essential mitotic checkpoint regulator that cooperates with Bub3 to prevent chromosome missegregation. *J. Cell Biol.* 160:341–353.

Bakkenist, C.J., and M.B. Kastan. 2003. DNA damage activates ATM through intermolecular autophosphorylation and dimer dissociation. *Nature.* 421:499–506.

Bartek, J., and J. Lukas. 2003. Chk1 and Chk2 kinases in checkpoint control and cancer. *Cancer Cell.* 3:421–429.

Bartkova, J., Z. Horejsi, K. Koed, A. Kramer, F. Tort, K. Zieger, P. Guldberg, M. Sehested, J.M. Nesland, C. Lukas, et al. 2005. DNA damage response as a candidate anti-cancer barrier in early human tumorigenesis. *Nature.* 434:864–870.

Burtelow, M.A., S.H. Kaufmann, and L.M. Karnitz. 2000. Retention of the hRad9 checkpoint complex in extraction-resistant nuclear complexes after DNA damage. *J. Biol. Chem.* 275:26343–26348.

Chen, Y., and Y. Sanchez. 2004. Chk1 in the DNA damage response: conserved roles from yeasts to mammals. *DNA Repair (Amst.).* 3:1025–1032.

Chini, C.C., and J. Chen. 2004. Claspin, a regulator of Chk1 in DNA replication stress pathway. *DNA Repair (Amst.).* 3:1033–1037.

Chini, C.C., and J. Chen. 2006. Repeated phosphopeptide motifs in human Claspin are phosphorylated by Chk1 and mediate Claspin function. *J. Biol. Chem.* 281:33276–33282.

Durkin, S.G., M.F. Arlt, N.G. Howlett, and T.W. Glover. 2006. Depletion of CHK1, but not CHK2, induces chromosomal instability and breaks at common fragile sites. *Oncogene.* 25:4381–4388.

el-Zein, R., P. Shaw, S.K. Tyring, and W.W. Au. 1995. Chromosomal radiosensitivity of lymphocytes from skin cancer-prone patients. *Mutat. Res.* 335:143–149.

Featherstone, T., A.M. Taylor, and D.G. Harnden. 1983. Studies on the radiosensitivity of cells from patients with basal cell naevus syndrome. *Am. J. Hum. Genet.* 35:58–66.

Feijoo, C., C. Hall-Jackson, R. Wu, D. Jenkins, J. Leitch, D.M. Gilbert, and C. Smythe. 2001. Activation of mammalian Chk1 during DNA replication arrest: a role for Chk1 in the intra-S phase checkpoint monitoring replication origin firing. *J. Cell Biol.* 154:913–923.

Goodrich, L.V., L. Milenkovic, K.M. Higgins, and M.P. Scott. 1997. Altered neural cell fates and medulloblastoma in mouse patched mutants. *Science.* 277:1109–1113.

Gorgoulis, V.G., L.V. Vassiliou, P. Karakaidos, P. Zacharatos, A. Kotsinas, T. Liloglou, M. Venere, R.A. Ditullio Jr., N.G. Kastrinakis, B. Levy, et al. 2005. Activation of the DNA damage checkpoint and genomic instability in human precancerous lesions. *Nature.* 434:907–913.

Gorlin, R.J. 1987. Nevoid basal-cell carcinoma syndrome. *Medicine (Baltimore).* 66:98–113.

Hahn, H., C. Wicking, P.G. Zaphiropoulous, M.R. Gailani, S. Shanley, A. Chidambaram, I. Vorechovsky, E. Holmberg, A.B. Unden, S. Gillies, et al. 1996. Mutations of the human homolog of *Drosophila* patched in the nevoid basal cell carcinoma syndrome. *Cell.* 85:841–851.

Hahn, H., L. Wojnowski, A.M. Zimmer, J. Hall, G. Miller, and A. Zimmer. 1998. Rhabdomyosarcomas and radiation hypersensitivity in a mouse model of Gorlin syndrome. *Nat. Med.* 4:619–622.

Hooper, J.E., and M.P. Scott. 2005. Communicating with Hedgehogs. *Nat. Rev. Mol. Cell Biol.* 6:306–317.

Jacob, L., and L. Lum. 2007. Deconstructing the hedgehog pathway in development and disease. *Science.* 318:66–68.

Jazayeri, A., J. Falck, C. Lukas, J. Bartek, G.C. Smith, J. Lukas, and S.P. Jackson. 2006. ATM- and cell cycle-dependent regulation of ATR in response to DNA double-strand breaks. *Nat. Cell Biol.* 8:37–45.

Johnson, R.L., A.L. Rothman, J. Xie, L.V. Goodrich, J.W. Bare, J.M. Bonifas, A.G. Quinn, R.M. Myers, D.R. Cox, E.H. Epstein Jr., and M.P. Scott. 1996. Human homolog of patched, a candidate gene for the basal cell nevus syndrome. *Science.* 272:1668–1671.

Karnitz, L.M., K.S. Flatten, J.M. Wagner, D. Loegering, J.S. Hackbarth, S.J. Arlander, B.T. Vroman, M.B. Thomas, Y.U. Baek, K.M. Hopkins, et al. 2005. Gemcitabine-induced activation of checkpoint signaling pathways that affect tumor cell survival. *Mol. Pharm.* 68:1636–1644.

Kimura, H., D. Stephen, A. Joyner, and T. Curran. 2005. Gli1 is important for medulloblastoma formation in Ptc1+/− mice. *Oncogene.* 24:4026–4036.

Lam, M.H., Q. Liu, S.J. Elledge, and J.M. Rosen. 2004. Chk1 is haploinsufficient for multiple functions critical to tumor suppression. *Cancer Cell.* 6:45–59.

Liu, Q., S. Guntuku, X.S. Cui, S. Matsuoka, D. Cortez, K. Tamai, G. Luo, S. Carattini-Rivera, F. DeMayo, A. Bradley, et al. 2000. Chk1 is an essential kinase that is regulated by Atr and required for the G(2)/M DNA damage checkpoint. *Genes Dev.* 14:1448–1459.

Olson, E., C.J. Nievera, V. Klimovich, E. Fanning, and X. Wu. 2006. RPA2 is a direct downstream target for ATR to regulate the S-phase checkpoint. *J. Biol. Chem.* 281:39517–39533.

Pandita, R.K., G.G. Sharma, A. Laszlo, K.M. Hopkins, S. Davey, M. Chakhparonian, A. Gupta, R.J. Wellinger, J. Zhang, S.N. Powell, et al. 2006. Mammalian Rad9 plays a role in telomere stability, S- and G2-phase-specific cell survival, and homologous recombinational repair. *Mol. Cell. Biol.* 26:1850–1864.

Pazzaglia, S., M. Mancuso, M.J. Atkinson, M. Tanori, S. Rebessi, V.D. Majo, V. Covelli, H. Hahn, and A. Saran. 2002. High incidence of medulloblastoma following X-ray-irradiation of newborn Ptc1 heterozygous mice. *Oncogene.* 21:7580–7584.

Pazzaglia, S., M. Tanori, M. Mancuso, M. Gessi, E. Pasquali, S. Leonardi, M.A. Oliva, S. Rebessi, V. Di Majo, V. Covelli, et al. 2006a. Two-hit model for progression of medulloblastoma preneoplasia in Patched heterozygous mice. *Oncogene.* 25:5575–5580.

Pazzaglia, S., M. Tanori, M. Mancuso, S. Rebessi, S. Leonardi, V. Di Majo, V. Covelli, M.J. Atkinson, H. Hahn, and A. Saran. 2006b. Linking DNA damage to medulloblastoma tumorigenesis in patched heterozygous knockout mice. *Oncogene.* 25:1165–1173.

Petermann, E., and K.W. Caldecott. 2006. Evidence that the ATR/Chk1 pathway maintains normal replication fork progression during unperturbed S phase. *Cell Cycle.* 5:2203–2209.

Roos-Mattjus, P., K.M. Hopkins, A.J. Oestreich, B.T. Vroman, K.L. Johnson, S. Naylor, H.B. Lieberman, and L.M. Karnitz. 2003. Phosphorylation of human Rad9 is required for genotoxin-activated checkpoint signaling. *J. Biol. Chem.* 278:24428–24437.

Ruiz i Altaba, A., C. Mas, and B. Stecca. 2007. The Gli code: an information nexus regulating cell fate, stemness and cancer. *Trends Cell Biol.* 17:438–447.

Sarkaria, J.N., E.C. Busby, R.S. Tibbetts, P. Roos, Y. Taya, L.M. Karnitz, and R.T. Abraham. 1999. Inhibition of ATM and ATR kinase activities by the radiosensitizing agent, caffeine. *Cancer Res.* 59:4375–4382.

Shafei-Benaissa, E., J.R. Savage, D. Papworth, P. Babin, M. Larregue, J. Tanzer, J.M. Bonnetblanc, L. Vaillant, and J.L. Huret. 1995. Evidence of chromosomal instability in the lymphocytes of Gorlin basal-cell carcinoma patients. *Mutat. Res.* 332:27–32.

Shafei-Benaissa, E., J.R. Savage, P. Babin, M. Larregue, D. Papworth, J. Tanzer, J.M. Bonnetblanc, and J.L. Huret. 1998. The naevoid basal-cell carcinoma syndrome (Gorlin syndrome) is a chromosomal instability syndrome. *Mutat. Res.* 397:287–292.

Syljuasen, R.G., C.S. Sorensen, J. Nylandsted, C. Lukas, J. Lukas, and J. Bartek. 2004. Inhibition of Chk1 by CEP-3891 accelerates mitotic nuclear fragmentation in response to ionizing radiation. *Cancer Res.* 64:9035–9040.

Volkmer, E., and L.M. Karnitz. 1999. Human homologs of *Schizosaccharomyces pombe* Rad1, Hus1, and Rad9 form a DNA damage-responsive protein complex. *J. Biol. Chem.* 274:567–570.

Wang, W.Y., M.T. Li, R.B. Pi, P.X. Qiu, X.W. Su, S.Z. Lin, and G.M. Yan. 2000. Antagonistic action of caffeine against LY294002-induced apoptosis in cerebellar granule neurons. *Acta Pharmacol. Sin.* 21:35–40.

Wang, X., L. Zou, H. Zheng, Q. Wei, S.J. Elledge, and L. Li. 2003. Genomic instability and endoreduplication triggered by RAD17 deletion. *Genes Dev.* 17:965–970.

Weiss, R.S., T. Enoch, and P. Leder. 2000. Inactivation of mouse *Hus1* results in genomic instability and impaired responses to genotoxic stress. *Genes Dev.* 14:1886–1898.

Wetmore, C., D.E. Eberhart, and T. Curran. 2000. The normal patched allele is expressed in medulloblastomas from mice with heterozygous germ-line mutation of patched. *Cancer Res.* 60:2239–2246.

Zhao, H., and H. Piwnica-Worms. 2001. ATR-mediated checkpoint pathways regulate phosphorylation and activation of human Chk1. *Mol. Cell. Biol.* 21:4129–4139.

Zou, L. 2007. Single- and double-stranded DNA: building a trigger of ATR-mediated DNA damage response. *Genes Dev.* 21:879–885.

Zou, L., D. Cortez, and S.J. Elledge. 2002. Regulation of ATR substrate selection by Rad17-dependent loading of Rad9 complexes onto chromatin. *Genes Dev.* 16:198–208.